

SIMULATIONS OF PRECIPITATE MICROSTRUCTURE EVOLUTION DURING HEAT TREATMENT

Kaisheng Wu¹, Gustaf Sterner², Qing Chen², Heng-Jeng Jou³, Johan Jeppsson², Johan Bratberg², Anders Engström², Paul Mason¹

¹Thermo-Calc Software Inc.;
4160 Washington Rd.; McMurray PA 15317, USA

²Thermo-Calc Software AB;
Norra Stationsgatan 93; SE 113 64 Stockholm, Sweden

³QuesTek Innovations LLC;
1820 Ridge Ave.; Evanston, IL 60201, USA

Keywords: Thermodynamics, Kinetics, Precipitation, Heat Treatment

Abstract

Precipitation, a major solid state phase transformation during heat treatment processes, has for more than one century been intensively employed to improve the strength and toughness of various high performance alloys. Recently, sophisticated precipitation reaction models, in assistance with well-developed CALPHAD databases, provide an efficient and cost-effective way to tailor precipitate microstructures that maximize the strengthening effect via the optimization of alloy chemistries and heat treatment schedules. In this presentation, we focus on simulating precipitate microstructure evolution in Nickel-base superalloys under arbitrary heat treatment conditions. The newly-developed TC-PRISMA program has been used for these simulations, with models refined especially for non-isothermal conditions. The effect of different cooling profiles on the formation of multimodal microstructures has been thoroughly examined in order to understand the underlying thermodynamics and kinetics. Meanwhile, validations against several experimental results have been carried out. Practical issues that are critical to the accuracy and applicability of the current simulations, such as modifications that overcome mean-field approximations, compatibility between CALPHAD databases, selection of key parameters (particularly interfacial energy and nucleation site densities), etc., are also addressed.

Introduction

The increasing interest in ICME techniques during recent years has boosted birth and maturity of efficient computational tools in a variety of industrial applications. TC-PRISMA[1] was developed to aid a systematic design of materials chemistry and heat treatments in order to achieve desired microstructures. It integrates seamlessly with THERMO-CALC[2] and DICTRA[2], and uses CALPHAD[3] databases for accurate thermodynamic and kinetic information in commercial alloys.

Recently, added functionality to simulate arbitrary heat treatment schedules, especially non-isothermal cooling conditions, has been included in TC-PRISMA. One of the most important applications of non-isothermal heat treatment is to produce complex multi-modal particle size distributions of γ' precipitates in Ni-base superalloys. The purpose of the current paper is to discuss this functionality and to evaluate its feasibility with several Ni-base alloys.

Model

TC-PRISMA has been developed based on Langer-Schwartz theory[4], and adopts Kampmann-Wagner numerical (KWN) method[5] for concurrent nucleation, growth, and coarsening of dispersed precipitate phases. The details of the employed model can be found elsewhere[1]. The major modification for non-isothermal conditions is the adoption of a transient nucleation model that calculates the incubation time as an integrated form of past thermal history[6]

$$\int_0^{\tau} \beta^*(t') dt' = \frac{1}{\pi Z^2(\tau)} \quad (1)$$

where τ is the incubation time, β^* is the impingement rate for solute atoms to the critical cluster, and Z is the Zeldovich factor.

TC-PRISMA uses CALPHAD databases for thermodynamic and kinetic data. In the current work, the thermodynamic database TTNi8[7] and the mobility database MOBNI1[2] have been used to carry out the simulations.

Results

Effect of Alloy Compositions: Ni-Al-Cr

In a recent paper, Rojhrunsakool et al. observed the composition dependence of the particle size distributions of γ' precipitates in Ni-Al-Cr alloys[8]. When subjected to the same continuous cooling condition, Ni-10Al-10Cr (at.%) alloy developed bimodal distribution of γ' precipitates, in contrast with Ni-8Al-8Cr where only single modal distribution occurred. In the current work, numerical experiments following their reported cooling treatment (continuous cooling from super-solvus temperature 1150°C to 380°C with a cooling rate of 14°C/min) have been performed. A constant interfacial energy of 0.023 J/m² has been used for these simulations. The results shown in Figure 1 clearly confirm their observations that Ni-10Al-10Cr generates a bimodal particle size distribution, whereas Ni-8Al-8Cr is of mono-modal type.

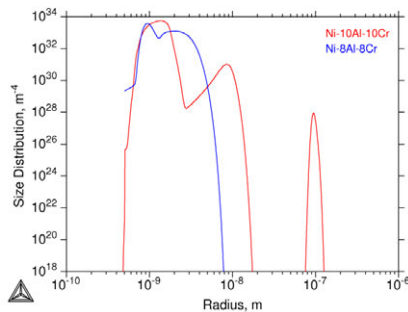


Figure 1 Calculated particle size distribution of γ' precipitates in Ni-10Al-10Cr and Ni-8Al-8Cr alloys after continuous cooling from 1150°C to 380°C with a cooling rate of 14°C/min

In-depth analyses of the simulation results have been carried out to gain more insight into the mechanisms that produce different γ' microstructures. The phase diagram in Figure 2(a) indicates

that Ni-10Al-10Cr has a higher solvus temperature than Ni-8Al-8Cr, which leads to a relatively rapid growth of primary γ' due to high atomic mobilities at high temperatures. Substantial growth of existing particles in Ni-10Al-10Cr results in severe drop of supersaturation of solutes in the matrix and brings down the driving force for nucleation to minimum values (see Figure 2(b)) so that the nucleation comes to halts (see Figure 2(c)). After each halt, further cooling increases the driving force gradually and gives rise to a new burst of nucleation when the driving force becomes large enough. In this way, multiple nucleation bursts can thus be produced, as shown clearly in Figure 2(c). For the alloy Ni-8Cr-8Ni, the nucleation of particles happens at relatively low temperatures and the growth of born particles is rather slow at low temperatures. As a result, the driving force available for nucleation is almost monotonically increasing during continuous cooling and no disruption of nucleation event occurs. Our quantitative analyses are in accord with the theoretical explanation which Rojhrunsakool et al.[8] gave to their experiments.

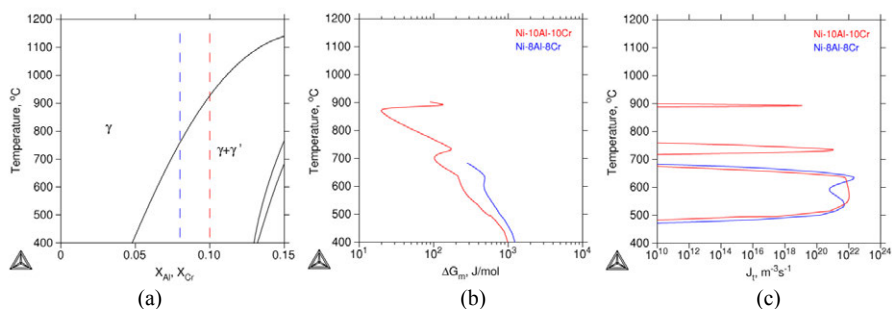


Figure 2 Calculated property diagrams in Ni-Al-Cr system. (a) phase diagram of Ni-xAl-xCr ($x=0-0.15$ at.%). (b) instantaneous driving force as function of temperature. (c) nucleation rate as function of temperature

Effect of Heat Treatments: U720Li Alloy

U720Li has been chosen to evaluate the feasibility of the current tool for practical applications. The main focus of the current work is on the formation of secondary and tertiary γ' , which are defined by superalloy society as γ' precipitates that form during continuous cooling. Meanwhile, all γ' particles are assumed to nucleate intra-granularly. The alloy compositions employed in the current work have been listed in Table 1, and their corresponding heat treatments in Table 2, on the basis of literature data[9-12]. A constant interfacial energy of 0.025 J/m^2 has been used to perform the simulation.

It can be seen from Table 2 that there are two types of heat treatments. The first one is continuous cooling from super-solvus temperature (Alloys 1 and 2), thus with an initial microstructure of pure γ matrix. Figure 3 illustrates the calculated variation of γ' particle size distributions with respect to the cooling rate. Within the studied cooling rate range, the results clearly indicate that decreasing cooling rate promotes the formation of multi-modal distributions, as the multiple peaks become more widely separated. Prolonged cooling time also results in larger particle sizes, as both secondary and tertiary γ' peaks shift to the right side. The plot of average size with respect to cooling rate further confirms this effect, as seen in Figure 4(a). It should be noted that the calculation of average size in Figure 4(a) has been conducted in

accordance with experimental methods which do not reflect the “actual” average size due to the complexity of the particle size distribution. Moreover, the calculations count only particles larger than 50nm, which was reported as their experimental limit[11]. One exception is those for small cooling rates ($< 0.2^{\circ}\text{C/s}$) where only secondary γ' particles have been considered. A higher calculated value is thus to be expected since some tertiary γ' might have been included experimentally. Despite this disparity, the overall agreements between calculated and measured results are very good. The linear relationship has been obtained when both size and cooling rate are in logarithmic scale, which agrees well with experimental observations[9-11] and other numerical simulations[9, 10].

Table 1 Compositions of U720Li Alloy (wt.%)

Alloy	Al	B	C	Co	Cr	Fe	Mo	Si	Ti	W	Zr	Ni
1[9, 10]	2.53	0.014	0.014	14.43	15.92	0.09	2.96		4.96	1.26		Bal
2[11]	2.46		0.025	14.75	16.35	0.06	3.02		4.99	1.3	0.035	Bal
3[12]	2.51	0.014	0.011	14.66	16.14		2.98	0.05	5.08	1.23		Bal

Table 2 Heat Treatments of U720Li Alloy

Alloy	Heat Treatment Conditions
1[9, 10]	Cooling from 1180 $^{\circ}\text{C}$ to 400 $^{\circ}\text{C}$ with varied cooling rates(0.217, 0.433, 0.867, 1.625, 3.25, 6.5, 19.5, 78 $^{\circ}\text{C/s}$)
2[11]	Cooling from 1175 $^{\circ}\text{C}$ to 650 $^{\circ}\text{C}$ with varied cooling rates(0.183, 0.46, 0.9417, 1.837, 2.86 $^{\circ}\text{C/s}$)
3[12]	Cooling from 1105 $^{\circ}\text{C}$ to 400 $^{\circ}\text{C}$ with varied cooling rates(20, 130, 280 $^{\circ}\text{C/min}$), followed by isothermal annealing at 700 $^{\circ}\text{C}$ for 24hrs

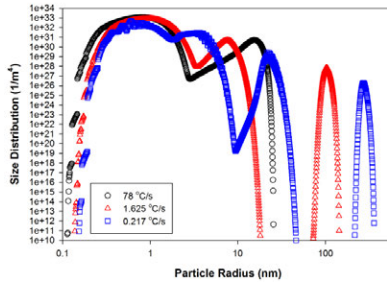


Figure 3 Simulation results for the effect of cooling rate on particle size distributions of γ' precipitates in U720Li Alloy 1

The other type of heat treatment is continuous cooling from sub-solvus temperature, followed by isothermal aging treatment (Alloy 3 in Table 2). In this case, we neglected the aging at 1105 $^{\circ}\text{C}$, prior to cooling, which produced primary γ' at grain boundaries[12], as the main focus was on the microstructure of secondary and tertiary γ' . Instead the primary γ' was assumed to reach its equilibrium fraction at 1105 $^{\circ}\text{C}$, and hence the γ matrix composition was adjusted accordingly based on equilibrium calculation. The results are compared with experiments[12] in Figure 4(b).

The same effect of cooling rate as for the previous simulation is observed. Again, satisfactory agreement has been obtained with exception for low cooling rates, where the calculation underestimated the size. This disagreement may arise from kinetic effect of preexisted primary γ' on the subsequent precipitation, which has been neglected in the current work. The grain boundary precipitation of secondary γ' can also be a factor.

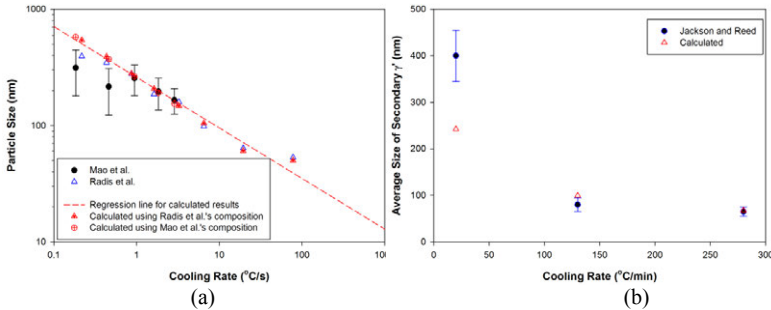


Figure 4 Comparison of calculated and experimental average γ' size as function of cooling rate. (a) with Alloy 1[9, 10] and 2[11]; (b) with Alloy 3[12].

Discussion

Most theoretical explanations attribute the multi-modal distribution during continuous cooling to the multiple distinct nucleation bursts caused by alternative dominance of nucleation driving force and solute depletion[9, 10, 13, 14]. Slow cooling promotes nucleation waves as the newly formed nuclei can have sufficient time to grow, draining solute atoms substantially until further nucleation appears upon subsequent cooling. The current model keeps abreast of the same physical background. Furthermore, it enables quantitative calculations, applicable to real alloy systems with the help of multi-component thermodynamic and mobility databases. Satisfactory agreements with experimental data have been obtained.

Some input parameters are known to have significant effect on the precipitation kinetics. First of all the accuracy and compatibility of thermodynamic and mobility databases are prerequisite to provide nucleation driving force and solute diffusivities. Secondly, interfacial energy is a key parameter, and unfortunately is difficult to obtain experimentally. Interestingly in the current work, interfacial energy seems relatively insensitive to the alloy composition and temperature. This thus makes it rather feasible for this tool to tailor alloy chemistry and heat treatment. Meanwhile, homogeneous intra-granular nucleation has been proven to be a reasonable approximation in most cases, except for those at very low cooling rate, where concomitant nucleation at multiple sites, e.g. at grain boundary and within the grain, is certainly a better option. The mean field approximation adopted in the current work is another source of uncertainty. It usually assumes a near zero volume fraction of precipitate phases. However, the presented simulation results indicate that it is still valid even for alloys with more than 40% of γ' phase, partly thanks to a modified growth model in terms of volume fraction. The mean field approach may also cause faster coarsening rate in multi-modal distributions. Fortunately, for the stage of continuous cooling in absence of a dominant coarsening process, this error is less severe than during long-time isothermal aging. Multi-type nucleation and growth rate modifications,

which have been under development, can be helpful to alleviate this error. Other microstructure complexities that affect the model accuracy, especially at very low cooling rates, include loss of coherency, varied interfacial energy, interface mobility, and morphology changes away from equiaxed shape, etc., which should be investigated in the future.

Summary

A non-isothermal model has been developed in TC-PRISMA and has been successfully applied to simulate multi-modal particle size distribution of γ' precipitates in Ni-base superalloys. In reasonably good agreements with experimental data, the simulations correctly predict the chemical and thermal conditions for mono- and bi-modal distributions, without requiring extensive use of adjustable parameters. The model proves to be valuable for designing alloy chemistry and heat treatment, but refinement is necessary for conditions that significantly deviate from mean field approximations.

References

1. Q. Chen et al. TC-PRISMA user's guide and examples. Thermo-Calc Software AB, Stockholm, Sweden, <http://www.thermocalc.se/Library.htm>; 2011.
2. Thermo-Calc Software AB. Stockholm, Sweden, <http://www.thermocalc.se/>.
3. N. Saunders, and A. P. Miodownik. *CALPHAD (Calculation of Phase Diagrams): A Comprehensive Guide*.(New York: Elsevier Science Ltd.; 1998).
4. J. S. Langer, and A. J. Schwartz. "Kinetics of nucleation in near-critical fluids", *Phys Rev A* 21(1980), 948-58.
5. R. Kampmann, and R. Wagner. "Kinetics of precipitation in metastable binary alloys - theory and application", *Decomposition of alloys: the early stages*, ed. P. Haasen et al.(Oxford: Pergamon Press, 1984), 91-103.
6. H. J. Jou et al. "Computer simulations for the prediction of microstructure/property variation in aeroturbine disks", *Superalloy 2004*. ed. K. A. Green et al. (Seven Springs, PA: TMS, 2004), 877-86.
7. N. Saunders et al. "The application of Calphad calculations to Ni-based superalloys", *Superalloys 2000*. ed. K. A. Green et al. (Warrendale, PA: TMS, 2000), 803-11.
8. T. Rojhirunsakool et al. "Influence of composition on monomodal versus multimodal γ' precipitation in Ni-Al-Cr alloys", *J Mater Sci* 48(2013), 825-31.
9. R. Radis et al. "Evolution of size and morphology of γ' precipitates in Udimet 720 Li during continuous cooling", *Superalloys 2008*. ed. R. C. Reed et al. (Seven Springs, PA: TMS, 2008), 829-36.
10. R. Radis et al. "Multimodal size distributions of γ' precipitates during continuous cooling of UDIMET 720 Li", *Acta Mater* 57(2009), 5739-47.
11. J. Mao et al. "Cooling precipitation and strengthening study in powder metallurgy superalloy U720LI", *Metall Mater Trans A* 32A(2001), 2441-52.
12. M. P. Jackson, and R. C. Reed. "Heat treatment of UDIMET 720Li: the effect of microstructure on properties", *Mater Sci Eng A* 259(1999), 85-97.
13. P. M. Sarosi et al. "Formation of multimodal size distributions of γ' in a nickel-base superalloy during interrupted continuous cooling", *Scripta Materialia* 57(2007), 767-70.
14. Y. H. Wen et al. "Phase-field modeling of bimodal particle size distributions during continuous cooling", *Acta Mater* 51(2003), 1123-32.